Time and spatial distribution of amplified acoustic flux in n-InSb

B. Fisher, B. Pratt, J. Gorelik, I. Feingold, and A. Many

Citation: Journal of Applied Physics **43**, 3607 (1972); doi: 10.1063/1.1661775
View online: http://dx.doi.org/10.1063/1.1661775
View Table of Contents: http://scitation.aip.org/content/aip/journal/jap/43/9?ver=pdfcov
Published by the AIP Publishing

Time and spatial distribution of amplified acoustic flux in n-InSb

B. Fisher, B. Pratt, J. Gorelik, and I. Feingold
Department of Physics, Techion-Israel Institute of Technology, Haifa, Israel

A. Many
The Racah Institute of Physics, The Hebrew University, Jerusalem, Israel
(Received 24 June 1971)

The growth process of amplified acoustic flux in n-InSb under an applied constant-current pulse is analyzed in detail, taking into account flux blocking and reflection at the contact-semiconductor interfaces. The analysis accounts well for the observed time and spatial distribution of the amplified flux, provided spurious effects associated with current feedback and hole injection is eliminated. The measurements provide conclusive evidence that the predominant source of the amplified flux in n-InSb is the thermal-equilibrium phonon distribution; the piezoelectric shock produced at the contact boundaries by the onset of the applied pulse plays no role in this respect. The information derived here on the detailed mechanism governing the flux growth is utilized in measurements of the gain parameters in InSb to be described in the following paper.

I. INTRODUCTION

Acoustoelectric amplification in n-InSb at 77 °K has been extensively investigated.[1,2] Most measurements were concerned with shear-wave propagation along the [110] direction, the orientation of strongest piezoelectric coupling. The interest in InSb stems largely from its high electron mobility (approaching 10^6 cm^2/V sec at 77 °K in some of the purer crystals). As a consequence, magnetic fields as low as several hundred G have a pronounced influence on the acoustoelectric gain, and interesting cyclotron-resonance effects are displayed. Another point of interest deriving from the high carrier mobility is that for the normally available samples (carrier concentration around 10^{14} cm^{-3}), the electron mean free path for scattering l is long compared to the mean wavelength λ of the *amplified* acoustic flux, i.e., $ql \gg 1$ (where $q = 2\pi/\lambda$). In this regime the gain mechanism is not collision dominated (as for the case of $ql \ll 1$), and one must use a microscopic theory[1] in describing the electron-phonon interaction.

In this and the following paper[3] we shall be concerned with acoustic amplification in InSb in the absence of a magnetic field. The present paper deals with the time and spatial distribution of the amplified acoustic flux, while in the second paper, measurements of the amplification factor are compared with the theory appropriate to that regime ($ql > 1$).

The main features of the acoustoelectric effect are most clearly displayed when the measurements are carried out under constant-current conditions (constant acoustic gain). One usually studies the time dependence of the voltage across the filament under constant-current pulses exceeding in amplitude the threshold for detectable acoustic gain. Typically (see, for example, Fig. 2 below), the filament voltage initially assumes an "Ohmic" value, followed by a gradual rise as the amplified acoustic flux becomes sufficient to increase the resistance of the sample. Finally, after about a sonic transit time, the filament voltage reaches a steady-state level, when the acoustic amplification is balanced by lattice attenuation and flux exit through the anode. This behavior indicates that the source of the amplified flux is the thermal-equilibrium phonon distribution. A simple analysis carried out by Bray, and based on uniform thermal generation of acoustic flux throughout the sample, accounts, at least qualitatively, for the main features of the time dependence of the filament voltage. Probe measurements of the electric-field distribution in the sample to be reported here provide more direct evidence that the amplified flux does indeed grow from the thermal background.

There is, however, one important aspect of the experimental results that cannot be accounted by Bray's simple model. One usually finds that the steady-state value of the filament voltage is not attained monotonically but is preceded by an "overshoot" (see Fig. 2 below). Bray[4] has attributed this behavior to impact ionization occurring in the high-field region of the filament (near the anode), where appreciable flux densities are built up. However, detailed probe measurements of the field distribution along the filament overrule this possibility except at extremely high gain levels (high currents). On the other hand, two other spurious processes can give rise to the overshoot, either jointly or separately. One is a feedback effect associated with departures from strict constant-current conditions. The other process is enhanced hole injection from the anode brought about by the increased electric field accompanying the amplified flux. Both these processes can be suppressed, if not entirely eliminated, by proper choice of the experimental conditions. Even then, however, an overshoot is still observed although its characteristics are different from those associated with feedback and injection. Our contention is that this overshoot originates from flux depletion at the cathode boundary on account of its blocking character. In Sec. II a detailed analysis of the flux-growth process is presented which takes into account such flux depletion. Experimental data pertaining to the field distribution along the filament and to the character of the overshoot are described in the following sections.

II. ANALYSIS OF FLUX-GROWTH PROCESS

Under thermal equilibrium, the flux density ϕ_0 in any given direction and at any frequency is maintained by balance between the thermal generation rate g and the attenuation rate. The latter rate can be expressed as $-(\alpha_0+\alpha_l)v_s\phi_0$, where α_l and α_0 are, respectively, the lattice and zero-field electronic attenuation factors per unit length. Hence the thermal generation rate of flux is given by[4]

$$g=(\alpha_0+\alpha_l)v_s\phi_0. \tag{1}$$

(The flux density ϕ is related to the acoustic energy density W by the relation $\phi = Wv_s$.)

Upon the application of a current pulse exceeding the threshold for net gain, the flux in and around the direction of electron drift will be amplified. Hence only flux propagating in a narrow cone (solid angle $\Delta\Omega$) along that direction need be considered. Furthermore, it will be sufficient to consider only the flux in a narrow bandwidth $\Delta\omega$ around the frequency of maximum gain. Henceforth ϕ (and ϕ_0) will denote the flux density in $\Delta\Omega\,\Delta\omega$. Small-signal conditions will be assumed such that the acoustic amplification factor α and the nonelectronic (lattice) attenuation factor α_l are independent of flux density. For n-InSb at 77 °K and not too high drift currents, α is very nearly given by[1]

$$\alpha\approx\alpha_0\gamma,\quad \gamma\equiv v_d/v_s-1, \tag{2}$$

where v_d is the electron drift velocity. For $v_d=0$, $\alpha=-\alpha_0$, where α_0 as defined above represents the zero-field electronic attenuation factor.

We consider now the flux-growth process following the onset (at $t=0$) of a constant-current pulse. At any time t shorter than the sonic transit time, only the flux originating *within* the filament can reach the points $x>v_st$ (where x is the distance from the cathode). Hence for a homogeneous sample the amplified flux density ϕ at all such points is uniform and is given by

$$\phi(x,t)=\phi_0\exp[(\alpha-\alpha_l)v_st]+\int_0^t g\exp[(\alpha-\alpha_l)v_s(t-t')]\,dt',\quad x>v_st. \tag{3}$$

The first term represents the amplified flux in a wave front starting at $t=0$ from the point $x-v_st$ (with initial level corresponding to the thermal density ϕ_0). The second term in Eq. (3) represents amplified flux added to this front as it propagates down the filament by thermal generation. By using Eq. (1) for g and carrying out the integration, one obtains

$$\phi(x,t)/\phi_0=[1+(\alpha_0+\alpha_l)/\alpha_n]\exp(\alpha_nv_st)-(\alpha_0+\alpha_l)/\alpha_n,\quad x>v_st \tag{4}$$

where $\alpha_n\equiv\alpha-\alpha_l$ is the net gain. Equation (4) is identical with that derived by Bray[4] for this regime.

For $x<v_st$, however, Eq. (3) must be modified in two respects: First, in order for the flux originating from the cathode boundary ($x=0$) to reach the point x at time t, it must leave this boundary at time $t-x/v_s$, when its density $\phi(0,t-x/v_s)$ may well be lower than ϕ_0 (see below). Second, this flux is amplified during the time interval of only $x/v_s(<t)$, so that the exponent of the first term in Eq. (3) must be changed into $(\alpha-\alpha_l)x$ while the limits of integration in the second term must be replaced by $t-x/v_s$ and t. Thus, analogously to the derivation of Eq. (3), one obtains

$$\phi(x,t)/\phi_0=[\phi(0,t-x/v_s)/\phi_0+(\alpha_0+\alpha_l)/\alpha_n]\exp(\alpha_nx)-(\alpha_0+\alpha_l)/\alpha_n,\quad x<v_st. \tag{5}$$

On the assumption that negligible flux is generated at the cathode boundary by the shock attending the onset of the pulse, there are two processes that can contribute to $\phi(0,t-x/v_s)$. One consists of transmission of thermal flux from the metal across the cathode boundary. This contribution amounts to $T\phi_0$, where T is the effective transmissivity of the boundary. The other contribution arises from back reflection of flux impinging on the cathode boundary from the semiconductor side. This impinging flux originates, as before, from thermal background. In this case, however, it propagates *against* the direction of electron drift and is therefore strongly attenuated. A calculation similar to that outlined above yields the same expression for the impinging flux as Eq. (4), provided $\alpha_n(\equiv\alpha-\alpha_l)$ is replaced by $-(\beta+\alpha_l)$, where β is the electronic attenuation factor for the upstream-propagating flux [$\beta\approx\alpha(1+2/\gamma)$, see Eq. (2)].

Thus, if R denotes the reflectivity at the cathode boundary, the downstream flux density at this boundary at any time t following the pulse onset is given by

$$\phi(0,t)/\phi_0=T+R\{[1-(\alpha_0+\alpha_l)/(\beta+\alpha_l)]\exp[-(\beta+\alpha_l)v_st]+(\alpha_0+\alpha_l)/(\beta+\alpha_l)\}. \tag{6}$$

Obviously, $T+R=1$. (In practice R is usually greater than T, most contacts being largely blocking to acoustic flux.) Using this relationship and substituting for $\phi(0,t-x/v_s)$ in Eq. (5) the expression derived from Eq. (6), one obtains

$$\phi(x,t)/\phi_0=[(\alpha+\alpha_0)/\alpha_n-R(\beta-\alpha_0)/(\beta+\alpha_l)]\exp(\alpha_nx)+R[(\beta-\alpha_0)/(\beta+\alpha_l)]\exp[-(\beta+\alpha_l)v_st+2(\beta-\alpha_0)x]-(\alpha_0+\alpha_l)/\alpha_n,\quad x<v_st. \tag{5'}$$

In n-InSb one usually has $v_d\gg v_s$, so that $\beta\approx\alpha$. Also, since the acoustic flux must be amplified several orders of magnitude above its thermal-equilibrium level before it becomes detectable, the term $(\alpha_0+\alpha_l)/\alpha_n$ can be neglected in Eqs. (4) and (5). Thus the flux distribution can be well approximated by

$$\phi(x,t)/\phi_0=(\alpha/\alpha_n)\exp(\alpha_nv_st),\quad x\geq v_st \tag{7}$$

$$\frac{\phi(x,t)}{\phi_0}=\frac{\alpha}{\alpha_n}\left\langle 1-R\frac{\alpha_n}{\alpha+\alpha_l}\{1-\exp[-(\alpha+\alpha_l)(v_st-x)]\}\right\rangle$$

$$\times \exp(\alpha_n x), \quad x \le v_s t. \tag{8}$$

In practice, one measures the excess (above-Ohmic) field $\Delta E(x, t)$ established in order to balance the acousto-electric field E_{ae} accompanying the acoustic flux. The relation between $\Delta E(x, t)$ and $\phi(x, t)$ is given by the Weinreich relation[5]

$$\Delta E(x, t) = (\alpha/ev_s n)\phi(x, t), \tag{9}$$

where e is the electronic charge and n is the electron concentration. Inspection of Eqs. (7) and (8) shows, then, that the excess field at any point x (as measured, for example, by a pair of potential probes) should exhibit the following behavior: It should first increase exponentially with time, reach a maximum at $t = x/v_s$ and then decay to a steady-state value. The rising and decaying exponentials are characterized by the time constants of $[(\alpha - \alpha_1)v_s]^{-1}$ and $[(\alpha + \alpha_1)v_s]^{-1}$, respectively. The ratio between the maximum and steady-state values is given by

$$\Delta E_{max}/\Delta E_{ss} = [1 - R\alpha_n/(\alpha + \alpha_1)]^{-1}. \tag{10}$$

Thus, for $R \neq 0$ one should observe the overshoot referred to above. The magnitude of the overshoot is expected to increase with applied current. [It can readily be shown that for the general case where β is not nearly equal to α, the term α in Eq. (10) should be replaced by β. In GaAs and particularly in CdS, $\alpha_n/(\beta + \alpha_1)$ is usually considerably smaller than the corresponding ratio in InSb so that the magnitude of the overshoot is expected to be much smaller.]

An additional contribution to the excess field comes about from reflection of flux at the *anode* boundary. The reflected flux ϕ_R propagates against the direction of electron drift, and its density at any time and any point in the filament is given by

$$\phi_R(x, t) = R\phi\{L, t - [(L - x)/v_s]\} \exp[-(\beta + \alpha_1)(L - x)], \tag{11}$$

where L is the filament length. It can readily be shown that for $\beta = \alpha$ one obtains

$$\phi_R(x, t)/\phi_0 = R(\alpha/\alpha_n)\exp[\alpha_n v_s t - 2\alpha(L - x)], \quad t \le (2L - x)/v \tag{12}$$

and

$$\phi_R/\phi_0 = R(\alpha/\alpha_n)[1 - R\alpha_n/(\alpha + \alpha_1)] \times \exp[-2\alpha_1 L + (\alpha + \alpha_1)x], \quad t \ge (2L - x)/v_s. \tag{13}$$

(For simplicity, the reflectivity of the anode is assumed to be the same as that of the cathode.) Since the reflected flux is attenuated, it gives rise to an acousto-electric field in the *same* direction as the field associated with the amplified downstream flux. This added field decays rapidly as one moves away from the anode so that it can be neglected over most of the filament. At the anode boundary itself, however, the added field is considerable. For $\beta \approx \alpha$, which is the case in n-InSb, the reflected flux doubles the field at the anode if $R = 1$, while in CdS, where $\beta \gg \alpha$, it may increase the field severalfold. This enhanced field can promote spurious effects such as hole injection from the anode, as will be discussed below.

The time dependence of the excess (above-Ohmic) filament voltage ΔV across the filament can be obtained by integrating Eq. (9) over the length of the sample. Consider first the time interval $0 \le t \le L/v_s$. For the downstream flux one has to use Eq. (8) for the filament section $0 \le x \le v_s t$ and Eq. (7) for the remainder of the filament. For the anode-reflected flux the integration should be carried out over the section $L - v_s t \le x \le L$ using Eq. (12). Neglecting again terms of the order of ϕ_0, one then obtains

$$\Delta V(t) = (1/ev_s n)(\alpha^2/\alpha_n^2)\phi_0[1 + \alpha_n(L - v_s t)]\exp(\alpha_n v_s t), \quad t \le L/v_s. \tag{14}$$

A similar procedure is used for $t > L/v_s$, leading to

$$\Delta V(t) = R^2(1/ev_s n)[\alpha/(\alpha + \alpha_1)]^2\phi_0[1 + (\alpha + \alpha_1)(v_s t - L)] \times \exp[-(\alpha + \alpha_1)v_s t + 2\alpha L] + (1/ev_s n)(\alpha/\alpha_n)^2\phi_0[1 - R^2\alpha_n^2/(\alpha + \alpha_1)^2] \times \exp(\alpha_n L), \quad t \ge L/v_s. \tag{15}$$

The time dependence of ΔV is similar to that of the excess field $\Delta E(x, t)$ [see Eqs. (7) and (8)]. Both exhibit

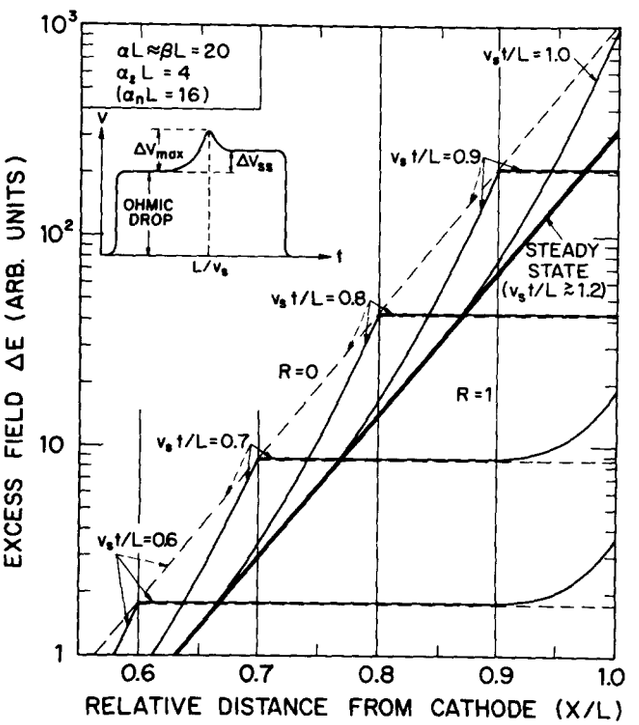

FIG. 1. Calculated excess-field distribution along filament at several instants following onset of acoustic gain. Dashed lines correspond to no reflection at cathode boundary ($R = 0$), while solid curves are for total reflection ($R = 1$). Effect of reflections at *anode* boundary are included only for two lower curves. Values for parameters αL and $\alpha_1 L$ are listed at top of figure. Schematic time response of filament voltage is also shown.

an overshoot, but in the case of ΔV the peak (which occurs at the sonic transit time from cathode to anode) is rounded off. Also, the ratio between the maximum and steady-state values of ΔV is smaller, being given by

$$\Delta V_{max}/\Delta V_{ss} = [1 - R^2\alpha_n^2/(\alpha + \alpha_l)^2]^{-1}. \quad (16)$$

The excess field distribution along the filament at several instants following the onset of the current pulse is illustrated in Fig. 1. The curves are based on Eqs. (7) and (8) for values of αL and $\alpha_l L$ typical to n-InSb at 77 °K. The dashed lines correspond to $R = 0$ (no flux reflection), while the solid curves are for total reflectivity of the cathode boundary ($R = 1$). In order not to overcomplicate the graphical presentation, the contribution from flux reflection at the *anode* boundary [Eqs. (12) and (13)] is included only for $v_s t/L = 0.6$ and 0.7. The marked changes in the field distribution brought about by flux reflection at the cathode is immediately apparent. At any given instant t, the flux density increases with distance faster than exponentially up to the point $x = v_s t$. From there the flux is uniformly distributed in a domain extending up to the anode. With time, the field distribution continuously changes form until shortly after the sonic transit time when the steady-state configuration is established (heavy line in Fig. 1). Whereas for $R = 0$, the flux at any point in the filament either remains constant or grows with time, for $R \neq 0$ the flux in the wake of the domain *decreases with time*. It is this behavior that can give rise to the observed overshoot in the time variation of ΔE and of $\Delta V (= \int_0^L \Delta E\, dx)$. The expected time response of the filament voltage to a constant-current pulse is shown schematically at the top left-hand corner of Fig. 1. The excess voltage ΔV reaches a maximum value at the sonic transit time (L/v_s) and then decays to its steady-state level.

III. EXPERIMENTAL

The electron concentration and mobility of the n-InSb samples studied (at 77 °K) varied in the ranges 8×10^{13}–8×10^{14} cm^{-3} and 7×10^5–2×10^5 cm^2/V sec, respectively. The filaments were cut along the [110] direction with typical dimensions of $20–30\times1\times1$ mm^3. After etching, end contacts and potential probes were attached to the filament by tellurium-doped indium solder. The probes were usually distributed along the filament in pairs, the probe diameter being a few tenths of a mm and the average distance about 1 mm. The samples were immersed in a liquid-nitrogen bath. All measurements were carried out with no applied magnetic field in order to avoid distortions in the electric field near the end contacts associated with the "geometrical magnetoresistance."[6,7]

A model 350 Velonex pulse generator was employed to provide the constant-current pulses through the filament. The voltage pulse was set at a maximum (2400 V), and the resistance in series with the filament was adjusted to obtain the desired current. The degree of constancy in the current obtained in this manner is at least $\Delta V_{max}/2400$, where ΔV_{max} is the maximum excess filament voltage. In some cases an electronic stabilizer fed by the voltage pulse was used to further enhance the current constancy.

Double current pulses were obtained from two Velonex pulse generators by a simple addition circuit. The time relation between the two pulses was adjusted by a suitable delay network.

The voltage across the filament and across the pairs of probes was displayed on a type 547 Tektronix CRO provided with a type 1A5 differential preamplifier. In the case of probe measurements a pair of attenuating probes was usually employed.

IV. RESULTS AND DISCUSSION

Typical oscillograms of the voltage across an n-InSb filament for a series of increasing constant-current pulses are shown in Fig. 2. The filament voltage is seen to rise gradually with time up to a peak value and then to decay towards a steady-state level. The overshoot peak occurs at the sonic transit time from cathode to anode and its magnitude increases with increasing current. Referring to the upper trace, one observes that the maximum change in filament voltage is 12 V, compared to the voltage pulse amplitude of 2400 V. Hence constant-current conditions are maintained to better than 0.5%.

The time variation of the voltage drop across a pair of close probes is shown in Fig. 3, again for a series of increasing constant-current pulses. The probes are located about 7 mm from the cathode, and the voltage drop across them represents the electric field at that point. (In this case, departures from constant-current conditions are less than 0.1%.) It will be noticed that the traces here are similar to those of the over-all filament voltage except that the overshoot peaks are considerably narrower. Also, now the peak occurs at the sonic transit time between the cathode and the probe location.

Probe measurements of the type shown in Fig. 3 were used to map out the spatial distribution of the electric field (and thus of the acoustic flux) along the filament.

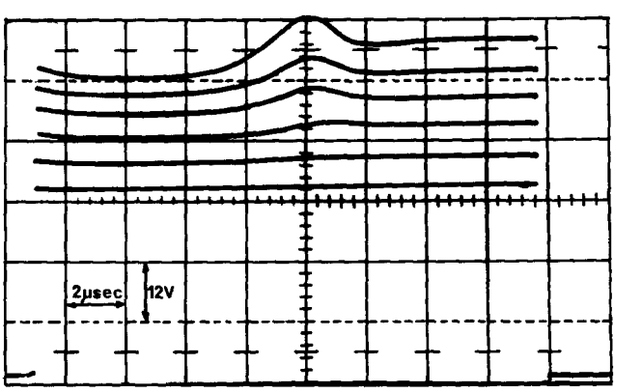

FIG. 2. Oscillogram traces of voltage across n-InSb filament (at 77 °K) for series of increasing constant-current pulses. Filament length 22 mm.

The filaments studied were carefully selected for homogeneity in resistivity. Semilog plots of the field distributions are shown in Fig. 4 for several instants following the onset of the constant-current pulse. For the particular value of the current applied, the flux reaches a detectable level after about 5 μsec, when it is nearly uniformly distributed in a domain extending over about one-half of the length of the filament (lower curve). The drop in flux density near the anode is due to the drop in resistivity in that region, as is verified by the measured resistivity profile of the filament. (Such degradation in resistivity was introduced by the prolonged heating of the anode contact found necessary in order to suppress hole injection.) The small variation in flux level in the plateau is believed to be likewise due to nonhomogeneities, in this case too small to be detected experimentally (less than 5%). The flux plateau rises (approximately exponentially) with time, but its left-hand edge is shifted to the right at sonic speed. The overshoot peak in Fig. 3 is a manifestation of this shift. It should be noted, however, that without the detailed mapping of the field distribution shown in Fig. 4, one might have interpreted traces like those in Fig. 3 as resulting from the propagation of a narrow domain originating at the cathode and superimposed on a broader distribution.

The most striking feature of Fig. 4 is that it provides conclusive evidence that the amplified flux in InSb originates entirely from the bulk thermal-equilibrium phonon distribution. From the observation that the flux distribution is not peaked at the points $x = v_s t$, one immediately concludes that the cathode does not act as a source of acoustic flux. At any instant t the flux plateau ($x \geq v_s t$), which encompasses most of the amplified flux, must have originated from points *within* the filament, where the only source of flux can be the uniform thermal background. The measurements to be described in the following paper[3] are based on this important conclusion.

As to the more detailed characteristics of the flux-growth process, Figs. 2–4 appear to be compatible with the results of the analysis presented above for the case in which the cathode boundary is largely blocking to flux

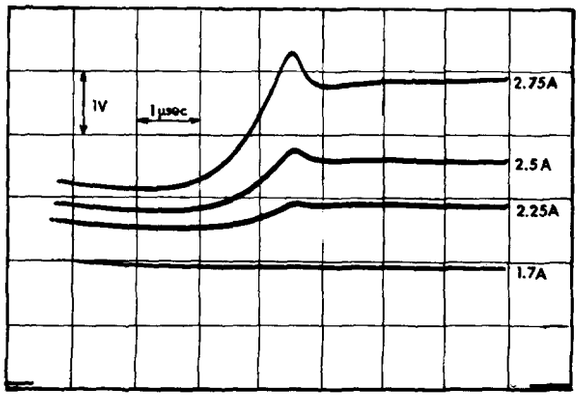

FIG. 3. Oscillogram traces of voltage drop across pair of probes for series of increasing constant-current pulses. Probes are approximately 1 mm apart and 7 mm from filament cathode.

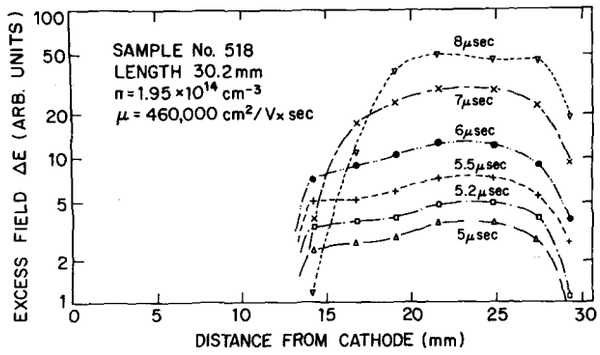

FIG. 4. Measured excess-field distribution along n-InSb filament for several instants following onset of constant-current pulse ($I = 7.3$ A, $\gamma = 70$).

incoming from the metal contact (see, e.g., the curves for $R = 1$ in Fig. 1). As will be shown below, however, other processes may give rise to a similar overshoot phenomenon. Accordingly, it is necessary to examine the data more closely before the role of flux blocking is definitely ascertained.

In principle, impact ionization occurring in the high-field flux domain can account[4] for the observed overshoot (as indeed it sometimes does at exceptionally high applied currents). Such a process can quench the high-resistance domain (without necessarily reducing appreciably the rate of flux growth) thereby giving rise to a drop in filament voltage towards some lower, steady-state level. Our data, however, overrule this possibility. Referring to Fig. 4, for example, one notes that the overshoot occurs while nowhere along the filament the excess electric field exceeds 50 V/cm. The Ohmic field in this case being 40 V/cm, it follows that the total field is well below the threshold for impact ionization (above 200 V/cm in our sample). In fact, in some cases an overshoot has been observed while the maximum local field was as low as 20 V/cm. Thus impact ionization does not play any role in the data presented.

A similar quenching of the high-resistance domain can occur by an entirely different process, namely, hole injection from the anode. The injection level should be expected to rise with increasing electric field at the anode and hence with increasing flux level. (As discussed above, back reflection of flux at the anode boundary would enhance this effect still further.) Thus, a point can be reached where the resistance quenching by injection predominates over the rise in acoustoelectric field due to the flux growth, and the filament voltage begins to *decrease* with time.

A feedback effect is another possible mechanism that can produce an overshoot. Unless constant-current conditions are strictly maintained, the increasing resistance of the filament associated with the growing flux will continuously reduce the current and hence the acoustic gain. Thus, flux arriving at a point x in the filament at sonic transit time x/v_s would have been amplified under somewhat higher gain than flux arriving at that point at a latter time ($t > x/v_s$). An upper limit

of this effect on the ratio between the peak (ΔV_{max}) and and the steady-state (ΔV_{ss}) excess filament voltage is readily obtained in the following manner: The gain determining ΔV_{max}, i.e., the gain during the interval $0 \le t \le x$, is taken as that corresponding to the initial Ohmic value of the current (actually the average gain is smaller), while the gain determining ΔV_{ss} is taken as that corresponding to the lower, steady-state current.

Whereas the amount of feedback can be suppressed or at least reliably estimated, the level of hole injection depends on the nature of the contact and is thus more difficult to control or evaluate. The effect of feedback has already been demonstrated by Bray[4] in a series of oscillograms obtained by a gradual transition from constant-current to constant-voltage conditions. The effect of injection is shown in Fig. 5, where measured values of $\Delta V_{max}/\Delta V_{ss} - 1$ are plotted on a semilog scale against the amplification factor α. The latter is proportional to the applied drift current [see Eq. (2)] and has been derived from measurements described in the following paper.[3] The maximum contribution of feedback under the conditions of the experiment is shown by the dashed line. It is seen to lie an order of magnitude below the measured points, so that feedback effects are negligible in this case. Yet, the experimental curve cannot be the result of flux blocking at the cathode over the entire range of the measurement. Referring to Eq. (16), one notes that $\Delta V_{max}/\Delta V_{ss}$ should increase slowly with increasing α. This is indeed the behavior exhibited by the results at low drift currents. At high α values, however, $\Delta V_{max}/\Delta V_{ss} - 1$ increases exponentially with α and is in fact proportional to the excess

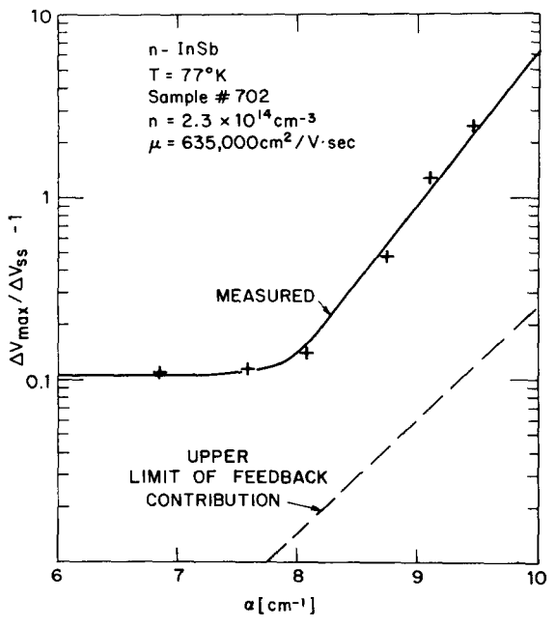

FIG. 5. Ratio of maximum (ΔV_{max}) to steady-state (ΔV_{ss}) excess filament voltage vs amplification factor α. Maximum contribution of feedback shown by dashed line. Slow variation of $\Delta V_{max}/\Delta V_{ss}$ -1 at low α attributed to flux depletion at cathode; exponential variation at larger α believed to be due to hole injection from anode.

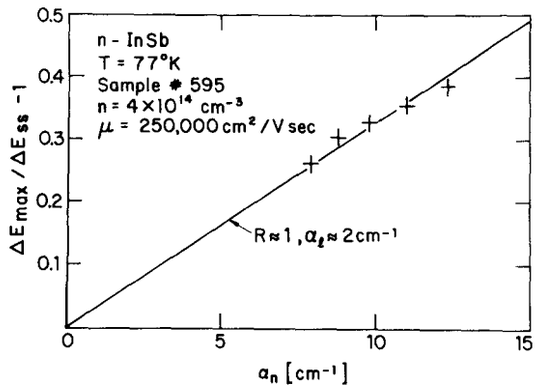

FIG. 6. Ratio of maximum (ΔE_{max}) to steady-state (ΔE_{ss}) excess field vs *net* amplification factor $\alpha_n (= \alpha - \alpha_l)$. Excess field measured across pair of probes approximately 1 mm apart and 7 mm from filament cathode. Effect of feedback and hole injection is negligible.

field at the anode boundary. This is just the behavior to be expected from injection quenching, and we believe that this process is the chief contributor to the observed overshoot in the high-current range.

In Fig. 6 probe measurements of $\Delta E_{max}/\Delta E_{ss} - 1$ are plotted (this time on a linear scale) against the *net* acoustic gain α_n. The maximum (ΔE_{max}) and the steady-state (ΔE_{ss}) excess fields refer to a point in the filament located 7 mm from the cathode. Here as well, feedback effects are negligible. Also, hole injection has been suppressed by prolonged heating during the formation of the anode contact. It is seen that in this case the points lie on a straight line which extrapolates to the origin, just as predicted by the analysis above [see Eq. (10)]. Furthermore, if total reflectivity ($R = 1$) is assumed, the value of α_l comes out to be about 2 cm^{-1}, which is the right order of magnitude for this type of sample.[3]

A further check on the validity of the analysis is provided by measurements of the time constants characterizing the rise and decay of the excess field on the two sides of the overshoot peak. The predicted time constants are $[(\alpha - \alpha_l)v_s]^{-1}$ and $[(\alpha + \alpha_l)v_s]^{-1}$, respectively. Considering, for example, the upper trace in Fig. 3, one derives (using higher gain and an expanded time scale) the values of about 10 and 15 cm^{-1} for $\alpha - \alpha_l$ and $\alpha + \alpha_l$, respectively. Thus $\alpha_l \approx 2.5$ cm^{-1}, which agrees well with our previous findings.

More direct evidence for the correlation between the overshoot and the process of flux blocking is provided by double-pulse measurements. The lower oscillogram in Fig. 7 displays the excess (above-Ohmic) voltage δV across a section of the filament near the anode for two consecutively applied constant-current pulses of equal amplitude. Following the onset of the first pulse, δV rises as usual towards a peak value and thence decays to its steady-state level, when the flux distribution along the filament is nearly exponential (see, e.g., Fig. 1). After the termination of the pulse, the flux is *uniformly* attenuated, maintaining its *exponential* dis-

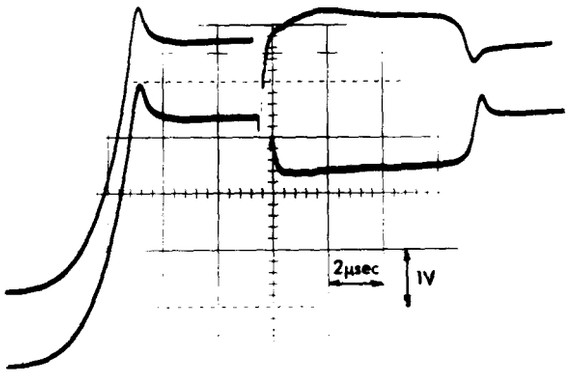

FIG. 7. Oscillogram traces of excess voltage across section of filament (2.5 mm) near anode for two consecutively applied constant-current pulses of equal amplitude. In lower trace the two pulses are separated by a short time interval, while in upper trace the two pulses overlap for a brief time.

tribution. Thus, when the second pulse is applied and acoustic amplification is restored, the flux density at any point well removed from the cathode does not change appreciably with time, until the flux originating near the cathode is amplified to a detectable level. At this point, the flux density rises and δV exhibits a similar behavior to that observed around a sonic transit time following the onset of the first pulse. However, the magnitude of the overshoot is somewhat smaller. This is because the time interval between pulses (when $v_d = 0$, $\alpha = -\alpha_0$) is not sufficient to restore fully the flux density at the cathode boundary to its thermal-equilibrium level ϕ_0.

An entirely different situation exists for the upper oscillogram. Here, the two current pulses are made to overlap slightly so that for a brief period the current amplitude is doubled. In this brief time interval the amplification factor α is enhanced, and as a result there is a small increment in the amplified flux level. By the same token, however, the attenuation factor $\beta(\approx \alpha)$ for the *upstream*-propagating thermal flux hitting the cathode is also enhanced [see Eqs. (11) and (12)]. This, in turn, results in further lowering of the back-reflected flux density at the cathode boundary during the overlap interval. The repercussion of such flux depletion at the cathode is revealed by the *undershoot*, which is seen to occur just a sonic transit time following the current-pulse overlap period.

V. CONCLUSION

The field-distribution measurements reported here leave little doubt that the predominant source of the amplified acoustic flux in n-InSb is the thermal-equilibrium phonon distribution. It has been established that the piezoelectric shock[8] produced at the contact boundaries by the onset of the applied pulse[9] plays little if any role in the flux-growth process. This is not really surprising if one bears in mind that in InSb appreciable acoustic gain is usually attained for applied fields as low as several tens of V/cm. In materials of lower mobility such as CdS, on the other hand, the applied field is considerably higher ($\approx 10^3$V/cm), as is the electromechanical coupling constant K^2, so that the shock is expected to be correspondingly greater. The relative importance of the two mechanisms in such materials is, however, still under debate.

Probe measurements of the field distribution in n-InSb have also been reported by Kikuchi *et al.*[10] and by Voges *et al.*[11] (In both cases the data were taken in the presence of a transverse magnetic field.) On the basis of double-pulse measurements, the former workers conclude that both shock-generated flux at the cathode boundary and thermal background contribute to the amplified flux. Our analysis, however, seems to account for their observations as well, and in view of the results presented here, we believe that the correct interpretation of their data also points to thermal background as the predominant source of the amplified flux. Voges *et al.*[11] observed nonuniform flux domains, several mm in width, propagating down the filament at sonic speed. Their measurements were carried out under nearly constant-voltage rather than constant-current conditions, so that feedback effects were prominent. Such feedback, combined with relatively small nonuniformity in the filament resistivity can account quite well for their observation. In fact, computer calculations of the amplified flux distribution under constant-*voltage* conditions and for a small (5–10%) linear decrease in resistivity between cathode and anode yield in typical cases curves for the field distribution similar to those reported by Voges *et al.*

The broader aspects of the observed field distribution under constant-current pulses can be accounted for by a simple analysis[4] based on *uniform* thermal generation of flux. Departures of the field distribution from the predictions of this analysis, exhibited more strikingly by the occurrence of an overshoot in local-field or filament-voltage oscillograms, indicate that other factors play a role as well in the flux-growth process. The evidence presented in this paper shows that if spurious effects associated with feedback and hole injection are eliminated, then the overshoot can be directly attributed to flux depletion at the cathode-InSb interface. Such depletion is a natural consequence of the blocking nature of the interface. The flux density at the interface following the onset of the current pulse is then controlled predominantly by the reflection of attenuated thermal flux impinging on the cathode from the semiconductor side. An analysis of the flux-growth process which takes into account such blocking and reflection at the interface accounts well for the experimental behavior.

ACKNOWLEDGMENTS

The authors are indebted to Z. Luz and Y. Shapira for helpful discussions and for their assistance in the calculations.

---

[1] J. Yamashita and K. Nakamura, *Proceedings of the Tenth International Conference on the Physics of Semiconductors, Cambridge, Mass., 1970*, edited by S.P. Keller, J.C. Hensel, and F. Stern (United States Atomic Energy Commission, Division of Technical Information, Washington, D.C., 1970), p. 694 (references).

[2]R. Bray, in Ref. 1, p. 705 (references).
[3]J. Gorelik, B. Fisher, B. Pratt, M. Zinman, and A. Many, J. Appl. Phys. **43**, 3614 (1972).
[4]R. Bray, IBM J. Res. Dev. **13**, 487 (1969).
[5]G. Weinreich, Phys. Rev. **107**, 317 (1957).
[6]G. Gorelik, M. Zinman, B. Fisher, and A. Many, J. Appl. Phys. **41**, 445 (1970).
[7]C. W. Turner, J. Appl. Phys. **39**, 4246 (1968).
[8]E. N. Jacobsen, J. Acoust. Soc. Am. **32**, 949 (1960).
[9]P. O. Silva and R. Bray, Phys. Rev. Lett. **14**, 372 (1965).
[10]M. Kikuchi, H. Hayakawa, and Y. Abe, Solid State Commun. **5**, 581 (1967).
[11]E. Voges, R. Jaenicke, and W. Harth, Arch. Elekt. Ubertragung **24**, 429 (1970).

Measurements of the acoustic gain parameters in *n*-InSb

J. Gorelik, B. Fisher, B. Pratt, and M. Zinman
Department of Physics, Technion-Israel Institute of Technology, Haifa, Israel

A. Many
The Racah Institute of Physics, The Hebrew University, Jerusalem, Israel
(Received 24 June 1971)

The drift-velocity dependence of the acoustic gain in *n*-InSb at 77 °K is derived from measurements of the rate of growth of the acoustoelectric field in the sample under constant-current pulses of different amplitudes. The amplified acoustic flux monitored by the acoustoelectric field originates from the thermal-equilibrium phonon distribution in the crystal. Results obtained for samples of different carrier concentrations are compared with the predictions of microscopic theories applicable to InSb ($ql > 1$). For low drift velocities the agreement between theory and experiment is very good. For drift velocities approaching the thermal velocity, on the other hand, the experimental data deviate markedly from the theoretical predictions. In this range appreciable carrier heating takes place, an effect that has not been adequately taken into account in the existing theories. The data also provide estimates for the nonelectronic (lattice) attenuation factor and for the initial thermal flux density. The values obtained for the latter are within an order of magnitude of those calculated on the basis of the thermal-equilibrium Debye spectrum.

INTRODUCTION

Indium antimonide constitutes a good medium for checking the validity of the microscopic theories[1-5] of acoustoelectric amplification in the regime $ql > 1$. An ideal tool for this purpose would have been Brillouin scattering, whereby the entire frequency spectrum of the amplified phonon distribution can be investigated. Since, however, InSb is transparent only at wavelengths exceeding 7 μ, such measurements are extremely difficult and as yet none have been reported. Several workers[6-8] employed transducers to inject into the sample acoustic flux at a single frequency and then measured the amplification as a function of drift current and magnetic field. This technique, while not easy, has great merit in that it permits, at least in principle, a point-by-point mapping of the frequency spectrum. So far, however, the amount of information available on the amplification process is still limited.

A simpler, if less direct, method of deriving the acoustic gain parameters is to amplify the thermal-equilibrium phonon distribution within the sample and use the acoustoelectric field as a monitor of the flux growth. This method, which consists essentially of analyzing the time variation of the acoustoelectric field for different applied constant-current pulses, is used in the present work. Prior knowledge of the laws governing the time and spatial distribution of the amplified flux is of course required. Such information is derived from the measurements and analysis discussed in the preceding paper, [9] which henceforth will be referred to as Paper I.

A disadvantage of this method is that a band of frequencies (around the frequency of maximum gain), rather than a single frequency, is involved in the amplification process. As will be discussed below, however, the bandwidth is relatively narrow and the gain parameters do not vary much over this bandwidth. The frequency of maximum gain is determined by the electron concentration, so that by using samples of different resistivities one can study the frequency dependence of the gain parameters.

Small-signal acoustoelectric amplification in the region $ql > 1$, including the effect of transverse magnetic fields, has been theoretically studied by a number of workers.[1-5] In fact, in most cases[1-4] generalized expressions have been derived for the amplification factor which are valid for any value of ql. For our purpose, however, it is sufficient to consider only the regime $ql \gg 1$, which is applicable to all our samples ($ql = 10$–15). Also, the discussion will be confined to zero magnetic field. Under these conditions ($ql \gg 1$, $B = 0$), one can easily check that the various theories yield much the same results. For sufficiently low drift currents the amplification factor (in units of reciprocal length) at any angular frequency ω is proportional to the electron drift velocity v_d and is given by[1,2]

$$\alpha(\omega) = (\pi^{1/2} K^2/v_T)(\omega^3/\omega_C\omega_D)(1+\omega^2/\omega_c\omega_D)^{-2}\gamma\,,$$
$$\gamma \equiv v_d/v_s - 1, \quad \omega_C = e\mu n/\epsilon, \quad \omega_D = ev_s^2/\mu kT\,, \tag{1}$$

where the symbols are defined as follows: K^2 is the electromechanical coupling constant, ϵ the static di-